

ChemComm

Accepted Manuscript



This is an *Accepted Manuscript*, which has been through the Royal Society of Chemistry peer review process and has been accepted for publication.

Accepted Manuscripts are published online shortly after acceptance, before technical editing, formatting and proof reading. Using this free service, authors can make their results available to the community, in citable form, before we publish the edited article. We will replace this *Accepted Manuscript* with the edited and formatted *Advance Article* as soon as it is available.

You can find more information about *Accepted Manuscripts* in the [Information for Authors](#).

Please note that technical editing may introduce minor changes to the text and/or graphics, which may alter content. The journal's standard [Terms & Conditions](#) and the [Ethical guidelines](#) still apply. In no event shall the Royal Society of Chemistry be held responsible for any errors or omissions in this *Accepted Manuscript* or any consequences arising from the use of any information it contains.

Cite this: DOI: 10.1039/c0xx00000x

www.rsc.org/xxxxxx

ARTICLE TYPE

Robust Pt-Sn Alloy Decorated Graphene Nanohybrid Cocatalyst for Photocatalytic Hydrogen Evolution

Chao Kong^{a,b}, Shixiong Min^{a,b}, Gongxuan Lu^{a}**Received (in XXX, XXX) Xth XXXXXXXXX 20XX, Accepted Xth XXXXXXXXX 20XX*

DOI: 10.1039/b000000x

The hydrogen evolution activity of Pt was remarkably enhanced by the addition of Sn species. The amount of H₂ evolution over the platinum tin alloy decorated graphene photocatalyst was 1.97 higher than that of Pt/Graphene in 90 min, and the highest apparent quantum efficiency reached 87.2% at 430 nm.

The photocatalytic hydrogen evolution from water splitting is an important process in sustaining solar energy conversion for the future¹. This process can be realized by using the photocatalytic hydrogen production system which usually contains a proton reducing catalyst, a photosensitizer and an electron donor². For efficient utilizing solar energy and enhancing the hydrogen evolution efficiency in these systems, many attempts have been devoted, including the application of the functionalized carbon materials to improve the charge separation efficiency³, extending the photoresponse range and applying highly active cocatalyst⁴. Among them, the high-efficient proton reducing cocatalyst is still critical factor for enhancing the hydrogen evolution efficiency⁵⁻⁷, and has got more attentions.

Noble metal Pt is high-efficiency hydrogen evolution cocatalyst because of its high activity and low overpotential for proton reduction, especially in neutral medium, but its high cost limits their potential wide applications⁸. So researchers focused on the searching of low-cost cocatalysts with comparative or even better catalytic activities than Pt. In the reported work so far, transition metals⁹, sulfides of transition metals^{7,9}, transition metal-based molecular complexes and their derivatives¹⁰⁻¹¹ are excellent cocatalyst for hydrogen evolution. However, these cocatalysts are often used in nonaqueous or non-neutral systems which are environmentally unfriendly.

Therefore, the enhancement of noble metal activity could be another promising route for the reduction of cost. In the present study, we remarkably improved the hydrogen evolution activity of Pt in the neutral mediums by the addition of other non-noble metal Sn species. The platinum tin alloy decorated graphene nanohybrid (Pt-Sn/G) was prepared by in-situ photoreduction deposition, which showed higher hydrogen evolution activity than Pt/G when sensitized by dye under visible light irradiation ($\lambda \geq 420$ nm). The amount of H₂ evolution over the EY-sensitized Pt-Sn/G system was 1331.8 μmol in 90 min, which was 1.97 higher than that of EY-Pt/G under the same reaction conditions, and the highest apparent quantum efficiency (AQE) of Pt-Sn/G reached 87.2% at 430 nm. It is noted that Pt-Sn nanohybrid had

comparative photocatalytic performance with Pt-Sn/G in triethanolamine (TEOA) aqueous solution (v/v = 10%, pH=7) under visible light irradiation. The excellent activities of Pt-Sn/G and Pt-Sn might be ascribed to the freshly generated hydrogen atom interfacial transfer from Pt to Sn site which is beneficial to desorption of H atom to produce H₂ quickly. To the best of my knowledge, Pt-Sn/G nanohybrid could be by far the highest active heterogeneous cocatalyst for photocatalytic hydrogen evolution in neutral solution.

Photocatalysts were synthesized by one-step photoreduction (see preparation details in ESI[†]). Transmission electron microscopy (TEM) image of Pt-Sn/G nanohybrid (Fig.1 A) displayed that the large amounts of nanoparticle adhered on the surface of graphene. Pt-Sn/G nanohybrid was further proved by high-resolution TEM (HRTEM) image. In Fig.1(B), the darker nanoparticle had the lattice spacing of 0.22 and 0.20 nm belonged to (102) and (110) planes of hexagonal PtSn¹², and the lighter with the interlayer distance of 0.33 and 0.26 nm was SnO₂¹³, which corresponded to the (110) and (101) planes of tetragonal SnO₂. The result indicated that the nanoparticles on the surface of graphene were Pt-Sn alloy and the crystalline SnO₂. The high angle annular dark field scanning transmission electron microscopy (HAADF-STEM) and elemental mapping characterization showed that the distribution of Sn and Pt element was relatively homogeneous in the lighter areas of HAADF-STEM image (Fig.1C). Fig.1(D), which was supported by the X-ray diffraction (XRD) patterns of Sn/Graphene (Sn/G), Pt/Graphene (Pt/G), Pt-Sn and Pt-Sn/G. In the diffraction spectrum of Sn/G, three peaks at 26.3°, 33.8° and 52.0° belonged to (110), (101) and (211) planes of tetragonal SnO₂ (JCPDS#77-0451), while the peaks at 29.5°, 31.8° and 44.7° could be assigned to (200), (101) and (211) planes of tetragonal Sn (JCPDS#89-4898). The result indicated that Sn/G nanocomposite contained the crystalline SnO₂. The weak diffraction peaks at 40.1° and 46.5° in XRD pattern of Pt/G belonged to (111) and (200) planes of cubic Pt (JCPDS#87-0647). The peaks of 26.3°, 33.8°, 51.9° and 64.8° in XRD pattern of Pt-Sn could be assigned to (110), (101), (211) and (112) planes of tetragonal SnO₂ (JCPDS#77-0451), and the weak peaks at 39.6°, 46.8° and 57.2° belonged to (200), (311) and (400) planes of cubic PtSn₂ (JCPDS#65-0960). In the diffraction spectrum of Pt-Sn/G, the weak peaks of 33.8° and 52.0° were identified as the (101) and (211) diffraction signals of SnO₂, and no diffraction peak of Pt appeared, implying the presence of Pt-Sn alloy in Pt-Sn/G nano hybrid^{12,14}. X-ray

photoelectron spectroscopy (XPS) of Pt-Sn/G (Fig.2A) exhibited that the Pt-Sn/G nanohybrid was mainly consisted of Pt, Sn, O and C elements. The binding energies of Sn 3d_{5/2} (487.2 eV) and Sn 3d_{3/2} (495.6 eV) in Fig. 2(B) indicated Sn element was in the +4 oxidation state of SnO₂, and the weak peaks at approximately 485.6 eV and 494.1 eV could be attributed to the presence of Sn metal. In Fig. 2(C), the peak at 70.9 eV could be assigned to Pt 4f_{7/2}, while the peak at 74.3 eV could be attributed to Pt 4f_{5/2}. The presence of both peaks at 70.9 and 74.3 eV indicated Pt element existed in the state of Pt metal in Pt-Sn/G nanohybrid. These results indicated Pt-Sn alloy and crystalline SnO₂ formed in Pt-Sn/G nanohybrid.

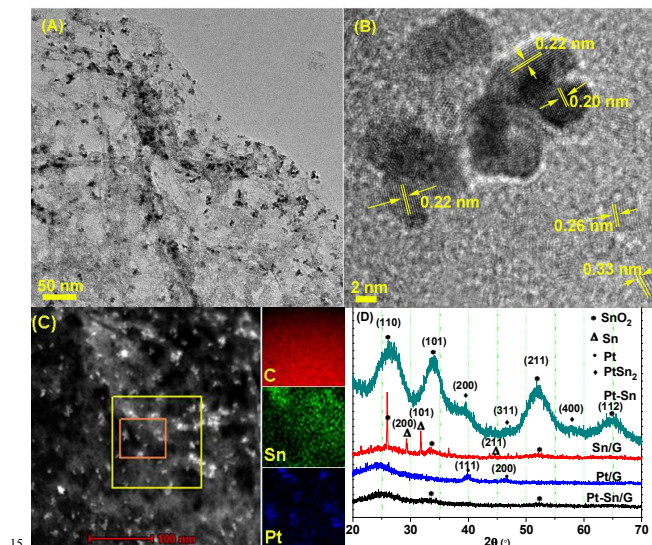


Fig.1 (A) TEM image and (B) HRTEM image for Pt-Sn/G nanohybrid; (C) HAADF-STEM (high angle annular dark field scanning transmission electron microscopy) image and elemental mapping images of Pt-Sn/G; (D) X-ray diffraction (XRD) patterns of Sn/G, Pt/G, Pt-Sn and Pt-Sn/G..

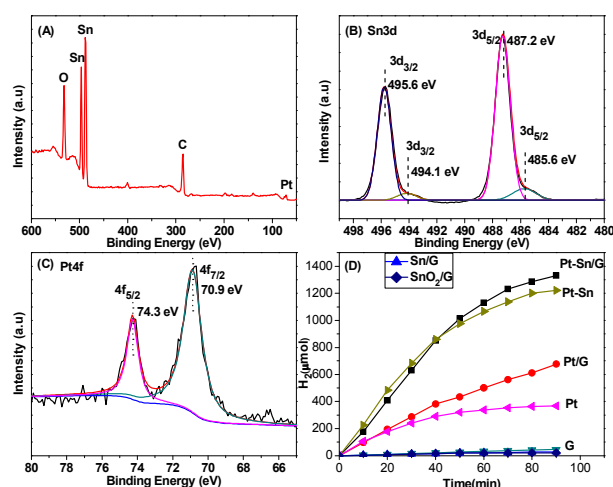


Fig. 2 (A) XPS survey spectra of Pt-Sn/G. (B) Sn 3d scan spectra of Pt-Sn/G. (C) Pt 4f scan spectra of Pt-Sn/G. (D) H₂ evolution from EY (1.0 × 10⁻³ mol/L) photosensitized systems catalyzed by Sn/G, G, Pt, Pt/G, Pt-Sn and Pt-Sn/G in 80 mL of 10% (v/v) TEOA aqueous solution (pH=7) under visible light irradiation

(λ ≥ 420 nm).

30

Fig. 2(D) showed the time courses of H₂ evolution catalyzed by graphene (G), Sn/G, Pt, Pt/G, Pt-Sn and Pt-Sn/G in 80 mL of 10% (v/v) TEOA aqueous solution (pH=7) under visible light irradiation (λ ≥ 420 nm). As can be seen from Fig.2(D), the small amounts of H₂ (45.5, 21.8 and 28.9 μmol) were generated over graphene, SnO₂/G and Sn/G cocatalyst after 90 min of irradiation, indicating that the graphene, SnO₂/G and Sn/G were low active for H₂ evolution. The hydrogen productions over EY-Pt-Sn photocatalyst was 1221.0 μmol in 90 min, which was 3.33 and 1.81 times higher than that of Pt (366.2 μmol) and Pt/G (676.3 μmol) under the same reaction conditions. Pt-Sn/G nanohybrid showed the highest photocatalytic performance, and the amount of H₂ evolution was 1331.8 μmol in 90 min, which was 1.97 higher than that of Pt/G (676.3 μmol) under the same reaction conditions. These results indicated the presence of Sn was crucial for improving the photocatalytic H₂ evolution activity of Pt/G and Pt. Graphene can facilitate the efficient electron transfer from photoexcited dye to the active sites and enhance photocatalytic hydrogen evolution activity by the prolongation of photogenerated electrons lifetime¹⁵⁻¹⁶. However, Pt-Sn composite had comparative photocatalytic performance with Pt-Sn/G in TEOA aqueous solution (v/v =10%, pH=7) under visible light irradiation. The likely reason is that SnO₂ nanoparticles on the surface of graphene in Pt-Sn/G might impede the efficient electron transfer of graphene to Pt-Sn active sites.

In photocatalytic hydrogen evolution process, these EY⁻ species which produced *via* the efficient intersystem crossing of singlet excited state EY^{1*} to EY^{3*} and the reductively quenching of EY^{3*} by TEOA subsequently could transfer their electrons to Pt-Sn nanoparticles, SnO₂ and graphene sheets. The accumulated electrons on the graphene sheets could transfer to Pt-Sn and SnO₂ sites, and electrons on SnO₂ sites might be quenched by TEOA⁺. H⁺ adsorbed on the surface of Pt could obtain electrons of Pt-Sn sites from EY⁻ and graphene to form hydrogen atom, which then could more easily desorb to produce H₂ quickly due to the existence of Sn^{13,17}(Scheme 1, ESI†). Therefore, Pt-Sn/G showed high photocatalytic activity for H₂ generation.

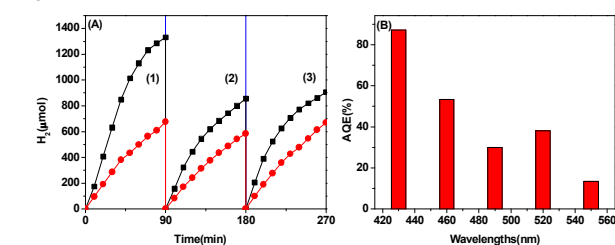


Fig.4 (A) Stability testing and compare of H₂ evolution over EY sensitized Pt/G (●) and Pt-Sn/G (■) in 80 mL of 10% (v/v) TEOA aqueous solution (pH=7) under visible light irradiation (λ ≥ 420 nm). The reaction was continued for 270 min, with evacuation every 90 min. (1) first run; (2) evacuation; (3) Pt/G and Pt-Sn/G were collected by centrifuging from reaction mixture. After washed thoroughly using deionized water, the recycled Pt/G and PtSn/G were mixed with TEOA solution and fresh EY, and evacuation. (B) Apparent quantum efficiencies (AQEs) of H₂ evolution catalyzed by Pt-Sn/G under light irradiation with

different wavelengths. The system was irradiated by a 300-W Xe lamp with a cutoff filter of 420 nm and a bandpass filter.

Irradiation time: 60 min.

The dependence of H₂ evolution activity on the weight ratio of Pt to Sn was investigated. Pt-Sn/G always showed good hydrogen evolution performance when mole ratio of Pt to Sn varied in range of 0.4/7 to 2.8/7, and the photocatalytic activity reached a maximum when the weight ratio of Pt to Sn was 1.2/7 (see Fig.S1, ESI†). The influence of the weight ratio of Pt-Sn to graphene on H₂ evolution activity was determined (see Fig.S2, ESI†), and the result indicated that the photocatalytic activity achieved a maximum when the weight ratio of Pt-Sn to graphene was about 1.37 and then reduce slightly with increasing the weight ratio of Pt-Sn to graphene further.

Furthermore, the stability test and compare of Pt-Sn/G and Pt/G has been carried out, and the result was shown in Fig.4(A). In the first run, the maximum photocatalytic H₂ production rate was 1384.8 μmol/h in the EY sensitized Pt-Sn/G hydrogen generation system. After evacuation, the maximum H₂ production rate of Pt-Sn/G system reached 939.6 μmol/h at the beginning of reaction in the second run. The reduction of H₂ production rate might be due to the decomposition of dye and sacrificial donor (Fig.S3, ESI†). The H₂ evolution activity of Pt-Sn/G could be revived to 68.2% by the concurrent addition of dye and TEOA in the third run, which still showed higher photocatalytic H₂ evolution activity than Pt/G. The dropping of Pt-Sn/G activity might be due to the loss of zero-valence Sn on the surface of Pt-Sn alloy (Fig.S4, ESI†).

Apparent quantum efficiencies (AQEs) of the EY-Pt-Sn/G system had also been examined under a wide range of visible light irradiation from 430 to 550 nm as shown in Fig.4(B). The highest AQE reached 87.2% at 430 nm due to the higher potential of photons, which was shorter than the wavelength of the highest absorption of EY (518 nm, Fig.S3, ESI†) in the visible light range. Pt-Sn/G had been shown to be an efficient electrocatalyst for the reduction of protons to molecular hydrogen based on the cyclic voltammetry (CV) study. As shown in Fig.5, the Pt-Sn/G/GCE electrode had the higher cathodic current beyond -0.7 V and lower onset potential of proton reduction than Sn/G/GCE and Pt/G/GCE electrode, which proved that Pt-Sn/G was remarkable cocatalysts which could efficiently catalyze the reduction of water to H₂.

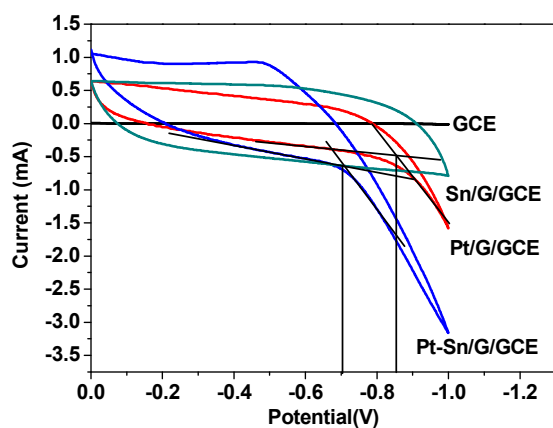


Fig.5 CV curves of GCE (Glassy carbon electrode), Sn/G, Pt/G/GCE and Pt-Sn/G/GCE electrode in 0.1 mol/L Na₂SO₄

solutions. The scan rate was 50 mV·s⁻¹.

In summary, Pt-Sn/G photocatalyst was synthesized by in-situ photoreduction deposition via Eosin Y photosensitizer in TEOA aqueous solution under visible light irradiation, which exhibited excellent photocatalytic performance in neutral medium when the weight ratios of Pt to Sn and Pt-Sn to graphene were 1.2/7 and 1.37 respectively. The hydrogen production over EY-Pt-Sn/G photocatalyst in 90 min was 1.97 higher than that of EY-Pt/G, and the highest apparent quantum efficiency (AQE) reached 87.2% at 430 nm. Moreover, this report will offer a new promising strategy to improve photocatalytic hydrogen evolution efficiency and reduce the cost.

This work is supported by the 973 and 863 Programs of Department of Sciences and Technology of China (2013CB632404, 2012AA051501) and the NSF of China (grant no. 21173242), respectively.

Notes and references

^aState Key Laboratory for Oxo Synthesis and Selective Oxidation, Lanzhou Institute of Chemical Physics, Chinese Academy of Science, Lanzhou 730000, China

^bUniversity of Chinese Academy of Science, Beijing 10080, China.

*Corresponding author: E-mail: gxl@lzb.ac.cn.

Tel.: +86-931-4968 178. Fax: +86-931-4968 178.

†Electronic Supplementary Information (ESI) available: [details of any supplementary information available should be included here]. See

DOI: 10.1039/b000000x/

- W. Zhang, J. Hong, J. Zheng, Z. Huang, J. Zhou, R. Xu, *J. Am. Chem. Soc.* 2011, **133**, 20680-20683.
- M. P. McLaughlin, T. M. McCormick, R. Eisenberg, P. L. Holland, *Chem. Commun.* 2011, 47, 7989-7991.
- S. Min, G. Lu, *J. Phys. Chem. C.* 2011, **115**, 13938-13945.
- S. Min, G. Lu, *J. Phys. Chem. C.* 2012, **116**, 19644-19652.
- M. G. Walter, E. L. Warren, J. R. McKone, S. W. Boettcher, Q. Mi, E. A. Santori, N. S. Lewis, *Chem. Rev.* 2010, **110**, 6446-6473.
- J. P. Bigi, T. E. Hanna, W. H. Harman, A. Changa, C. J. Chang, *Chem. Commun.* 2010, **46**, 958-960.
- S. Min, G. Lu, *J. Phys. Chem. C.* 2012, **116**, 25415-25424.
- H. Yan, J. Yang, G. Ma, G. Wu, X. Zong, Z. Lei, J. Shi, C. Li, *J. Catal.* 2009, **266**, 165-168.
- C. Kong, S. Min, G. Lu, *Int. J. Hydrog. Energy.*, 2014, **39**, 4836-4844.
- O. Pantani, S. Naskar, R. Guillot, P. Millet, E. A. Mallart, A. Aukauloo, *Angew. Chem. Int. Ed.*, 2008, **47**, 9948-9950.
- L.A. Berben, J.C. Peters, *Chem. Commun.*, 2010, **46**, 398-400.
- C. Hsieh, Y. Chang, K. Yin, *J. Phys. Chem. C.* 2013, **117**, 15478-15486.
- C. Kong, S. Min, G. Lu, *Chem. Commun.*, 2014, **50**, 5037-5039.
- C. Hsieh, Y. Liu, W. Chen, Y. Hsieh, *Int. J. Hydrog. Energy.*, 2011, **36**, 15766-15774.
- Q. Xiang, J. Yu, M. Jaroniec, *J. Am. Chem. Soc.*, 2012, **134**, 6575-6578.
- I.V. Lightcap, T.H. Kosel, P.V. Kamat, *Nano Lett.* 2010, **10**, 577-583.
- G. Jerkiewicz, *Prog. Surf. Sci.*, 1998, **57**, 137-186.

Novel platinum tin alloy decorated graphene nano hybrid (Pt-Sn/G) as robust photocatalyst exhibited higher hydrogen evolution activity than Pt/G under visible light irradiation.

